ELSEVIER

Journal of Structural Geology 30 (2008) 29–38

JOURNAL OF STRUCTURAL GEOLOGY

www.elsevier.com/locate/jsg

Thrust initiation and propagation during shortening of a 2-layer model lithosphere

Fernando O. Marques*

Facultad de Ciências, Departamento de Geologia and IDL, Universidade Lisboa, Edificio C6, Piso 2, 1749-016 Lisbon, Portugal

Received 2 June 2007; received in revised form 17 September 2007; accepted 19 September 2007
Available online 29 September 2007

Abstract

Analogue modelling was used to investigate thrust initiation and propagation in the lithosphere. The model comprised a top layer of light sand (model brittle crust) overlying a layer of heavy silicone putty (model ductile lower crust), both resting upon higher density and lower viscosity natural honey (model ductile mantle). The experiments show the following. (1) Thrust initiation may occur in two main modes: fold-first or fault-first. They seem to be the result of presence or absence of an initial perturbation close to the piston, respectively. The fault-first mode eventually goes into a fold-first mode after a certain amount of deformation. (2) In both modes, thrusts localized around the inflection points of both fore and back-limbs of buckles as a result of tectonic (horizontal), gravitational (vertical) and elastic forces. (3) Thrust propagation in the fault-first mode occurred by thrust wedge thickening and downward flexure due to isostatic compensation, which led to forward formation of bulges and subsequent amplification by buckling. Continued shortening increased the stresses that reached the brittle yield of sand and new thrusts originated. (4) Bulging ahead of thrusts tended to develop into asymmetric buckles with the shorter limb (back-limb) steeper towards the piston. (5) As a whole, thrust initiation and propagation seem to depend mostly on how stresses evolve and propagate through the model and how material strength varies with progressive deformation. The main stresses at play are born at the moving piston (model horizontal tectonic force), from thickening and isostatic compensation in the model (gravitational forces), and from elastic resistance to buckling.

Keywords: Shortening; Lithosphere instability; Buckling; Thrust initiation; Thrust evolution and propagation; Gravitational forces

1. Introduction

Vening-Meinesz (1958), based on the strength of the lithosphere, suggested that excessively large forces are required to buckle the crust. Later, Ramberg and Stephansson (1964) used analytical and experimental approaches to show that the crust as a whole is not capable of responding to lateral stress by buckling of geosynclinal dimensions. In contrast, for example Lambeck (1983) and McAdoo and Sandwell (1985) showed that buckling of continental or oceanic lithosphere is possible. This could be the case of deformation far from plate boundaries in the oceanic lithosphere of the Central Indian Ocean (e.g. Weissel et al., 1980; McAdoo and Sandwell, 1985; Cloetingh and Wortel, 1986; Gerbault et al., 1999; Gerbault, 2000) or of the Eurasian plate north of the Asia/India boundary (e.g. England and Jackson, 1989; Stephenson and Cloetingh, 1991; Burg et al., 1994; Cloetingh et al., 1999; Burg and Podladchikov, 1999; Schmalholz et al., 2002). Cobbold and Davy (1988), Davy and Cobbold (1988, 1991), Burg et al. (1994), Gerbault et al. (1999) and Sokoutis et al. (2005) investigated the behaviour of n-layered models of the lithosphere and concluded that thrusts initiate at inflection points of buckles. By analogue modelling, Shemenda (1992) investigated the behaviour of the lithosphere under horizontal compression; the lithospheric model was 1-layer (plastic layer on top of water) and there was no erosion or sedimentation. The results show both fold-first and fault-first modes, but the author did not discuss why. Martinod and Davy (1994) investigated periodic instabilities during shortening of the lithosphere and also observed that buckling preceded thrusting, but also did not discuss initiation

* Tel.: +351 217 500 000; fax: +351 217 500 064.
E-mail address: fomarques@fc.ul.pt

0191-8141/$ - see front matter © 2007 Elsevier Ltd. All rights reserved.
doi:10.1016/j.jsg.2007.09.005

and propagation of thrust faults. In contrast, Gerbault et al. (1999) concluded from a numerical study that, under reasonable tectonic stresses, folds might develop from brittle faults cutting through the brittle parts of the lithosphere, although they also say that folding and faulting may happen simultaneously.

It is apparent from the existing literature that the development of periodic instabilities in the lithosphere, in particular the timing of buckling and thrusting, is still not well understood. The objective of the present work has been, therefore, to investigate where, when and how thrusts initiate and propagate, and their relationship with buckling. For this, analogue modelling was used with materials appropriately scaled for nature and gravity. Thrusting in a thick skin model is investigated. However, not so thick as to root thrusting in a deep asthenosphere/lithosphere interface as done in 4-layer models of the lithosphere. Thrusts in the present models root at the Moho. At this stage of the experimental study, erosion and sedimentation (e.g. Lambeck, 1983; Koyi et al., 2000; Marques and Cobbold, 2006), or more than a 2-layer lithosphere are not introduced, to avoid undesirable complexity of models and variables. Hence the effects of two main forces can be investigated, horizontal (model tectonic forces) and vertical (model gravitational forces), and mechanical properties of the materials without manipulation of erosion and deposition loci.

2. Experimental method

The relationship between stress and strain depends upon many variables, which are in part unknown or may vary both spatially and temporally. However, for practical purposes, it seems reasonable to consider the rheology of the continental lithosphere in a simplified manner, by means of a strength profile (e.g. Goetze and Evans, 1979; Kusznir and Park, 1982; Kirby, 1983; Carter and Tsenn, 1987). According to experimental and theoretical studies, the upper crust yields by brittle failure, so that its strength increases with depth. In contrast, the lower crust and much of the mantle seem to yield by viscous flow, so that creep strength depends mostly upon temperature. On this basis, Davy and Cobbold (1991) showed that, for high thermal gradients, the resistance of the ductile upper mantle is almost negligible. Hence, for the purposes of the present investigation, one brittle layer and one viscous layer adequately represent a high thermal gradient continental crust, resting upon an upper mantle of lower viscosity, as done by Davy and Cobbold (1991) and Martinod and Davy (1994). Besides, it has been shown that model lithosphere with more layers brings more complexity to the experimental results, but not significant differences regarding thrust initiation and/or evolution. Therefore, a 2-layer model of the lithosphere is used. Additionally, with such a set up, the oceanic lithosphere is also modelled.

2.1. Scaling

The models were at lithospheric scale, so that gravity played an important role as in nature. The basal low viscosity layer guaranteed isostatic compensation and topography could develop freely. Following Davy and Cobbold (1988, 1991), a length ratio $\lambda = l_{\text{model}}/l_{\text{nature}} = 6.67 \times 10^{-7}$ was chosen, so that a continental crust, 30 km thick, scaled down to a model layer ca. 20 mm thick. The models were 500 mm long, 480 mm wide and 80 mm deep (Fig. 1), representing $750 \times 720 \times 120$ km in nature. To represent the brittle upper crust, a granular material was used, for which cohesion was negligible and the angle of internal friction was between 30° and 40°, as in brittle rock (Hubbert, 1937, 1951). Appropriate low strength of the ductile layer requires low strain rates and thus the application of small model/nature time ratios. Following Davy and Cobbold (1988), a time ratio of 1.0×10^{-10} was used (1 hour representing about 1 Ma). This gave a velocity ratio of 5.33×10^{3}, so that a natural velocity of about 8 cm a^{-1} (convergence rate between Nazca and South American plates) scaled down to 1.39×10^{-5} m s^{-1} in the models. Because inertial forces were negligible, the viscosity ratio equalled the product of density, length and time ratios (Hubbert, 1937), becoming $(0.4) \times (6.67 \times 10^{-7}) \times (1 \times 10^{-10}) \approx 2.7 \times 10^{-17}$. The density ratio is found by dividing the density of the PDMS mixture (ca. 1.2×10^{3} kg m^{-3}) by the density of the lower crust (ca. 3.0×10^{3} kg m^{-3}). Therefore, to represent a lower crustal layer having a viscosity of about 10^{21} Pa s, a model material with a viscosity of about 4×10^{4} Pa s was used.

2.2. Model materials

In order to model the brittle upper crust, natural quartz sand from Fontainebleau (Krantz, 1991) was used. The grain size is about 300 μm, and the density about 1.3×10^{3} kg m^{-3}. The density was reduced to about 1.15×10^{3} kg m^{-3} by admixture of ethyl cellulose powder. The mixture fails according to a Navier–Coulomb frictional law, and it has negligible cohesion and an angle of internal friction of about 40°.

For the viscous lower crust, a mixture of PDMS (95% by weight) and fine haematite powder (5%) was used. The PDMS was the variety SGM36, manufactured by Dow-Corning Inc. At room temperature, this material has a density of 0.965×10^{3} kg m^{-3}. At low strain rates, it has a small but

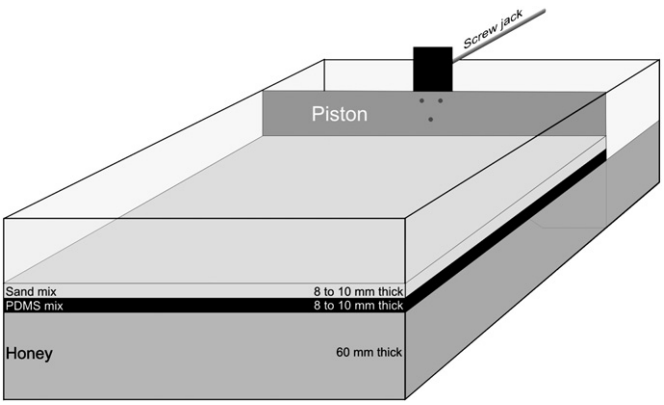

Fig. 1. Schematic oblique view of apparatus and model.

significant elastic response; otherwise it behaves as a Newtonian fluid with a viscosity of about 10^4 Pa s (Weijermars, 1986). The PDMS-haematite mixture has a density of about 1.2×10^3 kg m^{-3}. Tested in a thick-walled rotary viscometer and compared with pure SGM36, it shows less of an elastic response, is closer to Newtonian and has a somewhat smaller viscosity. For the mantle, a natural clear honey was used. This material behaves as a Newtonian fluid, and it has a density of about 1.35×10^3 kg m^{-3} and a viscosity of about 10 Pa s. Using the above viscosity ratio, it is apparent that this viscosity is too low when scaled up to nature. However, Davy and Cobbold (1991) showed that the resistance of the ductile upper mantle is almost negligible for high thermal gradients; hence a weak fluid is used, whose main role is to provide isostatic support.

2.3. Apparatus and boundary conditions

The models were constructed and then deformed in a rectangular box (Fig. 1). Its walls were fixed, except one (piston), and made of transparent material (Perspex). A computer-controlled stepping motor drove the piston at a steady velocity of 1.39×10^{-5} m s^{-1}, so shortening the model. There was frictional resistance at the sidewalls, because PDMS adhered to Perspex and the coefficient of sliding friction for sand against Perspex is significant. However, the width of the box is large when compared to model crust thickness (25 to 1); hence boundary effects are not expected to significantly influence stress and strain distribution throughout the model, or overall structural style and evolution. Anyway, attention was paid to lateral boundary effects during the experiments. PDMS drag and sand friction on sidewalls impede rigorous measurements, such as detailed evolution of sand and PDMS thickness during deformation (localized or diffuse). Despite blurring, overall geometry and evolution is visible through sidewalls.

Two types of initial set up were investigated. (1) One in which some extra sand was allowed to accumulate close to the piston, making a small wedge due to PDMS sinking. This wedge was almost flat at the surface, but dipped gently (ca. 10°) towards the piston at the sand/silicone interface. The width of the wedge, measured orthogonal to piston, was between 20 and 30 mm. Therefore, there was an initial perturbation, but only in the contact with the piston. (2) Another setup in which this wedge did not exist at the initial stage, hence the layers were flat and orthogonal to piston, with no intentional and perceptible perturbation added to the initial model.

3. Experimental results

Faults, folds and horizontal displacements were monitored using digital time-lapse imaging under low-angle lighting. Displacement vectors were constructed as in Marques and Cobbold (2002). Both plan views (vertical images) and side views (through the transparent sidewalls) were used. At the end of each experiment, the sand layer was vacuumed off to reveal the upper surface of the PDMS. In the following, the limbs of buckles are denoted as forelimb and back-limb; the back-limb is closer to and faces the piston, and the forelimb is further and looks away from piston.

Two main modes of deformation timing were found in the experiments, which will be called fold-first or fault-first, depending on whether folding precedes faulting or vice-versa, respectively.

3.1. Fold-first

We do not elaborate much on this mode because the present results are similar to published work. At the initial stage, there was a perturbation close to piston. At the early stages of compression, the model lost stability and buckling formed ahead of the piston. Before the first thrust formed, several buckles developed but gradually died out away from the piston (Fig. 2). The average initial wavelength was ca. 80 mm and the wavelength over thickness ratio was about 8 (80 mm/10 mm). Using the adopted length ratio $\lambda = 6.67 \times 10^{-7}$, 80 mm scale up to about 120 km in nature. Continued compression increased the amplitude of buckles and reduced their wavelength. At a certain stage, a fore-thrust nucleated somewhere in the mid part of the forelimb of the more amplified, closer to piston buckle. Later in the experiments, back-thrusts also formed. Similar behaviour has been reported by Cobbold and Davy (1988), Davy and Cobbold (1991), Cobbold et al. (1993), Martinod and Davy (1994), Burg et al. (1994) and Sokoutis et al. (2005), who presumed that thrusts were born at inflection points of buckles or at sags (Shemenda, 1992). In Section 4 below, an alternative location for thrust initiation (although in the forelimb) is presented and a physical mechanism is proposed to explain fore-thrust initiation in the forelimb of buckles.

3.2. Fault-first

At the onset of shortening there was no intentional perturbation or weakness; hence layers were flat and horizontal to the naked eye, and compression was transmitted to the entire model. At the initial stages of compression, the entire sand/PDMS pack shortened and thickened. However, displacement gradually died out towards the wall opposite to piston (cf. displacement vectors in Fig. 3), and so did thickening. This was more prominent close to piston, in the form of a wedge, and soon deformation localized as a fore-thrust that developed immediately ahead (Fig. 3A). With continued shortening, this thrust took up most shortening imposed by piston displacement (cf. displacement vectors in Fig. 3B), and the thrust wedge thickened. Because the model was isostatically compensated, (1) the light underthrusted sand exerted a vertical, upward force (buoyancy) on the overlying thrust slice; (2) the hanging wall rose appreciably forming a prominent fault scarp (cf. Figs. 3 and 4); (3) the thrust fault became listric (steeper close to the surface and gradually decreasing dip with depth toward piston); (4) the sand/PDMS pack bent downward; and (5) a bulge formed ahead of the thrust (fore

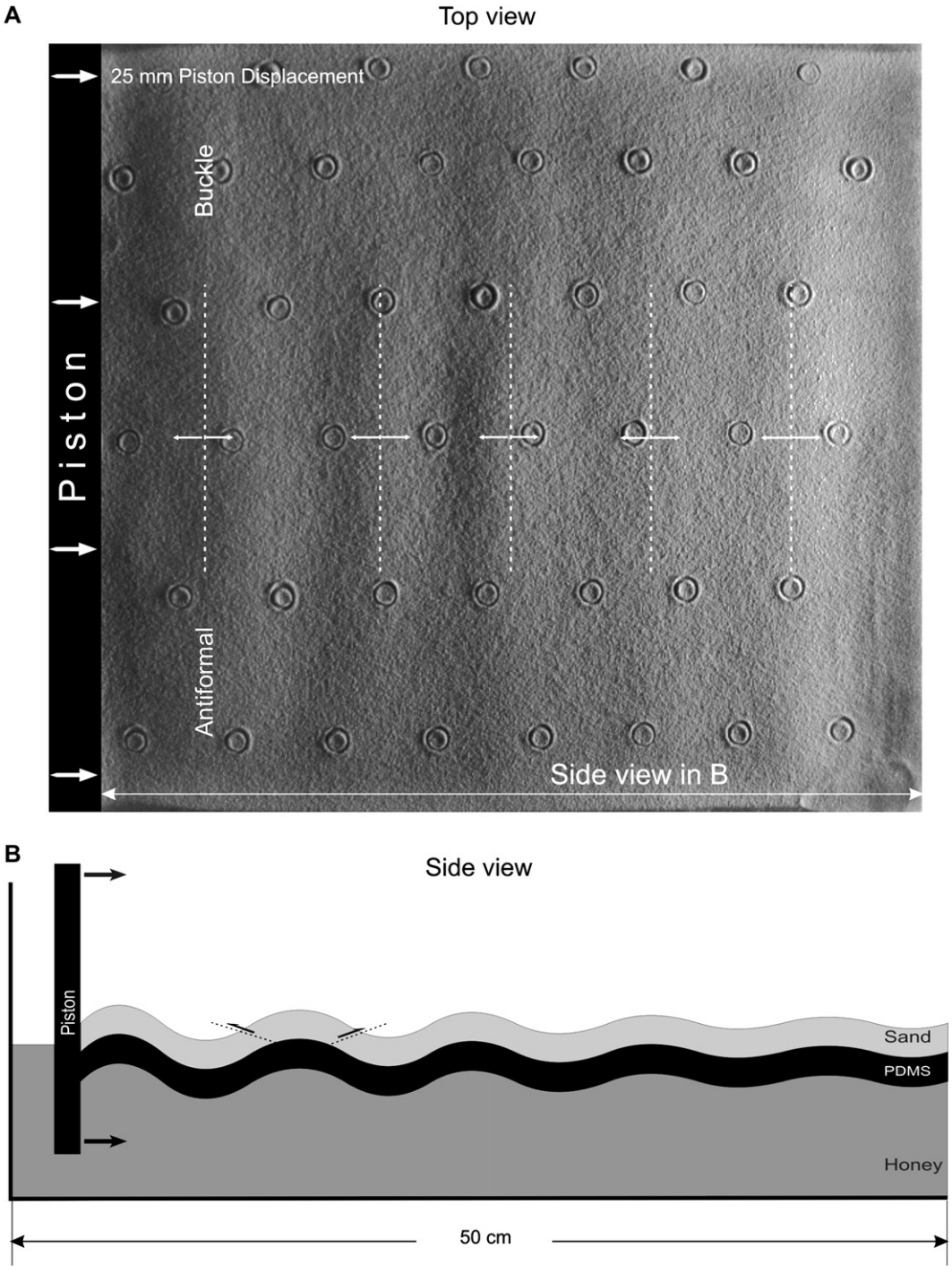

Fig. 2. Deformation after 25 mm piston displacement, in fold-first mode. Rectilinear piston moved from left to right at steady velocity. (A) Plan view photograph (under low-angle lighting from the right) shows structures at upper surface of model. Free surface was initially flat and horizontal, and there was no erosion or sedimentation during the run. Buckling propagated from left to right and died out in the same sense. (B) Sketch of side view.

bulge in Figs. 3A, 4 and 5A). The approximate wavelength to (initial) thickness ratio of the fore bulge was 12, because the model wavelength was about 120 mm, which scales up to a natural wavelength of ca. 180 km. The fore bulging provided the perturbation sufficient to develop a buckle with further shortening. Amplification of this buckle initiated a first cycle of fold-first sequence; hence a new fore-thrust developed from forelimb of the buckle (Fig. 3B). Because the ductile layer was also buckled, thrusting in sand dragged a thin sheet of silicone into the hanging wall of the thrust (Fig. 4), thus weakening the fault zone and making it more localised and more long-lived (e.g. Koyi et al., 2000). With continued shortening and isostatic compensation, the model crust bent and another asymmetric, piston verging bulge formed. Following further shortening, a buckle amplified in front of the fore-thrust (Fig. 3C). After some buckle amplification, two thrusts

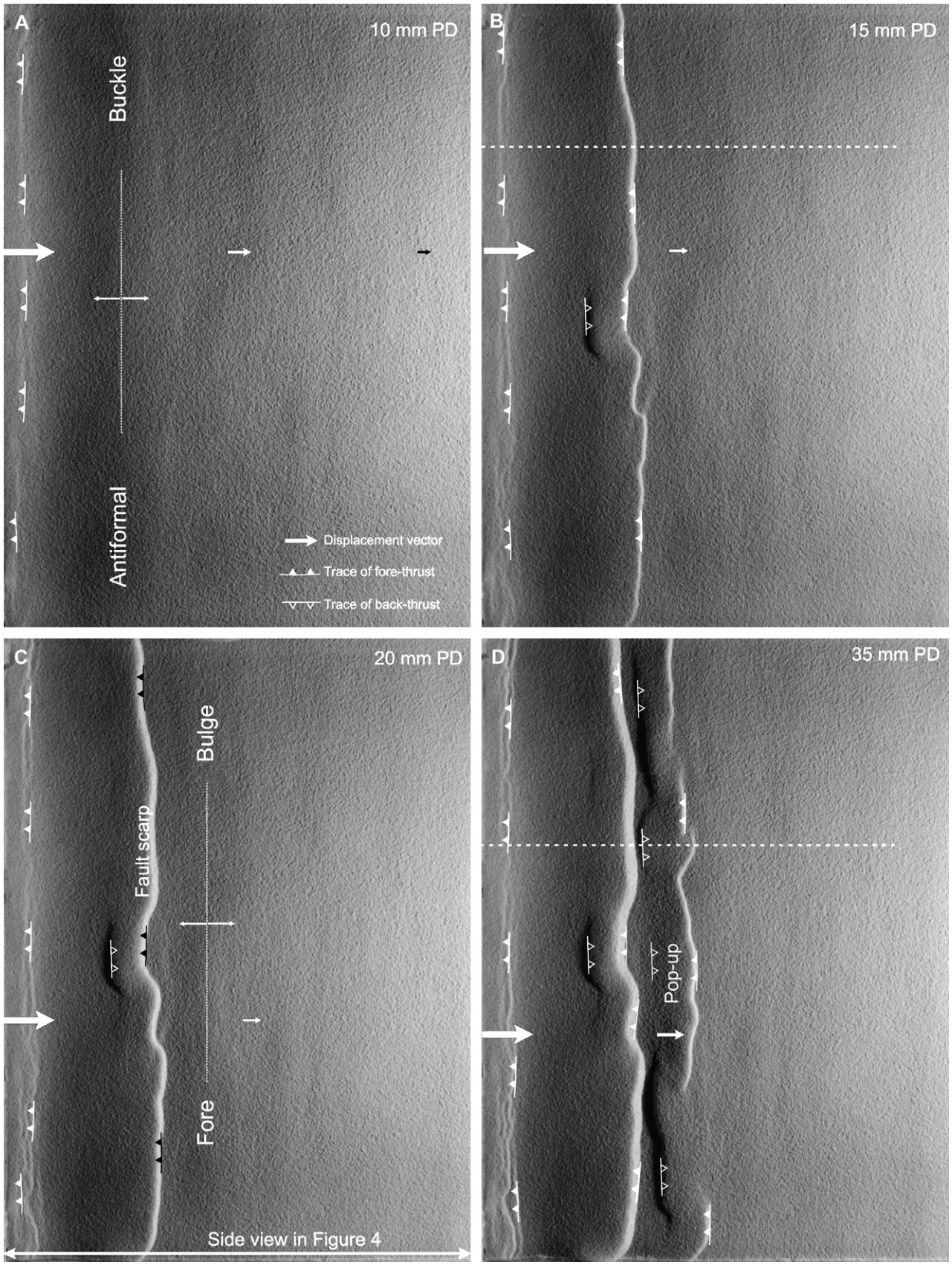

Fig. 3. (A–F) Six stages of deformation for fault-first mode. Plan view photographs (under low-angle lighting from the right) show structures at upper surface of model, for six values of piston displacement (PD). Free surface was initially flat and horizontal and there was no erosion or sedimentation. Structures propagated from left to right. Dashed white lines in B and D mark locations of sketch sections represented in Fig. 5.

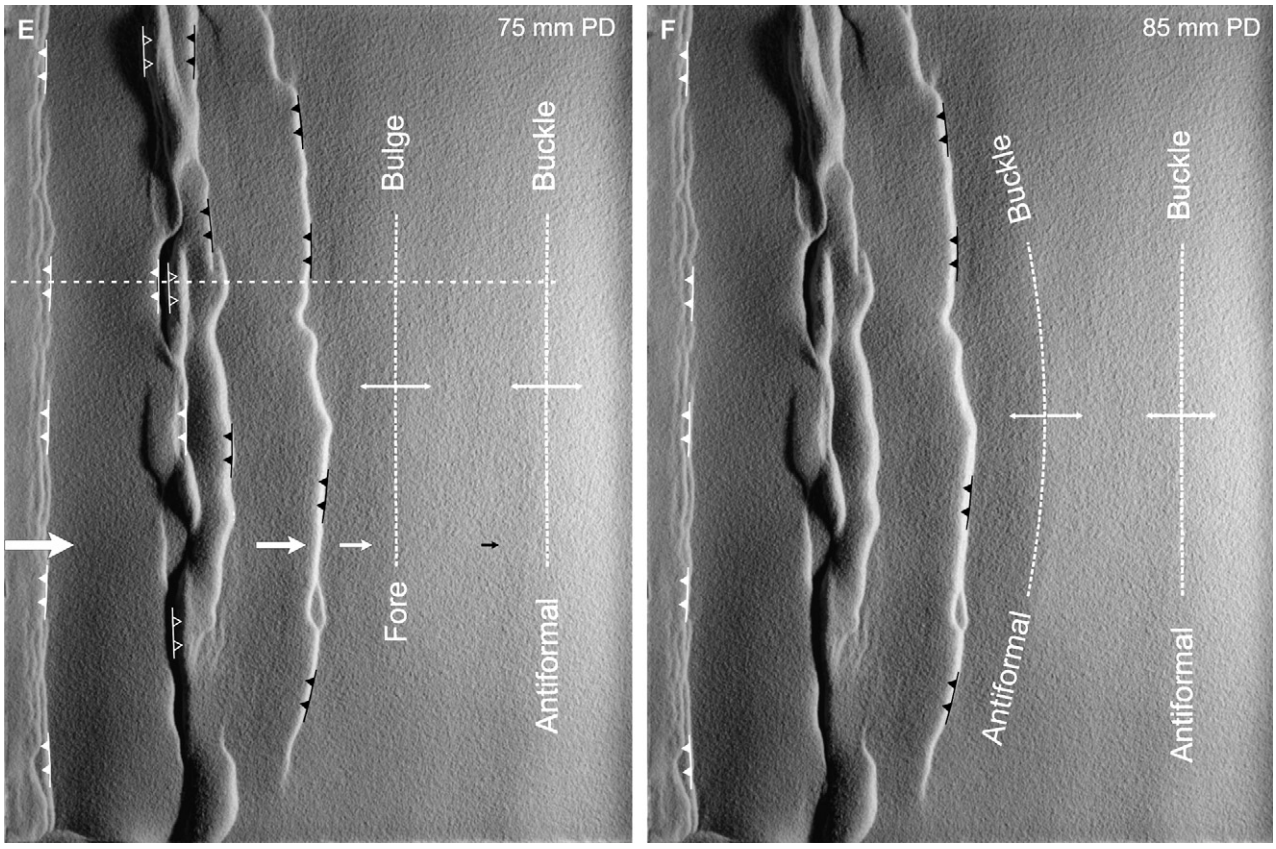

Fig. 3 (*continued*).

formed simultaneously from this fold, but one was a back-thrust and the other a fore-thrust (Figs. 3D and 5B). This latter lasted for a very short time, while the back-thrust took up most deformation and formed a contractional basin with the earlier fore-thrust (Fig. 3E). Only after a great deal of shortening (ca. 70 mm piston displacement) a new fore-thrust formed from the forelimb of a new bulge-then-buckle that formed ahead of the contractional basin (Fig. 3E and F).

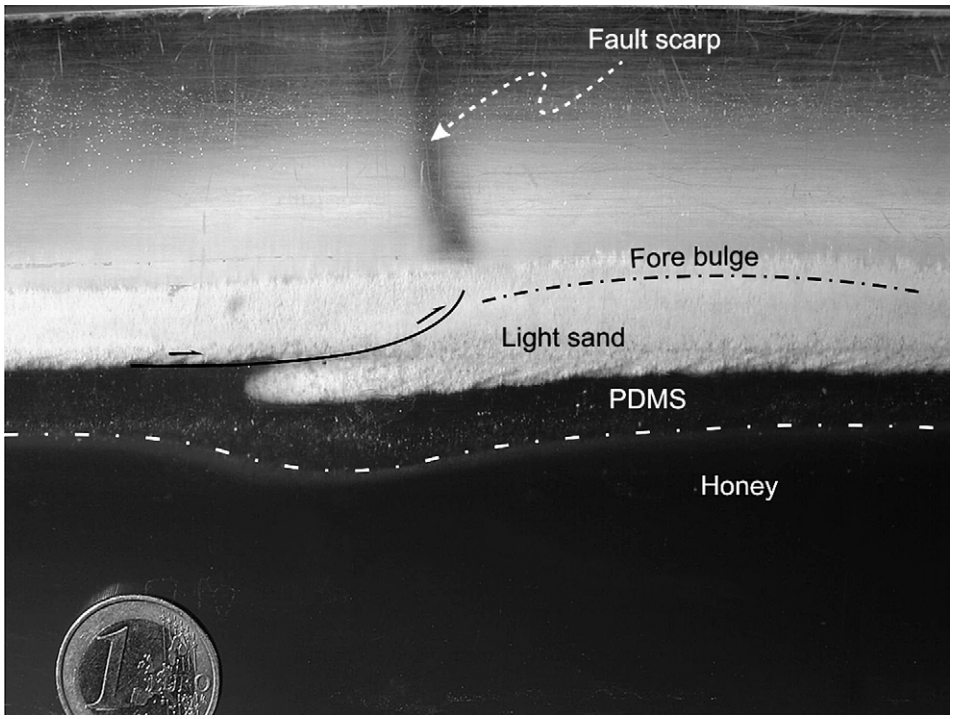

Fig. 4. Photograph of sidewall view of fault-first experiment, with piston moving from left to right.

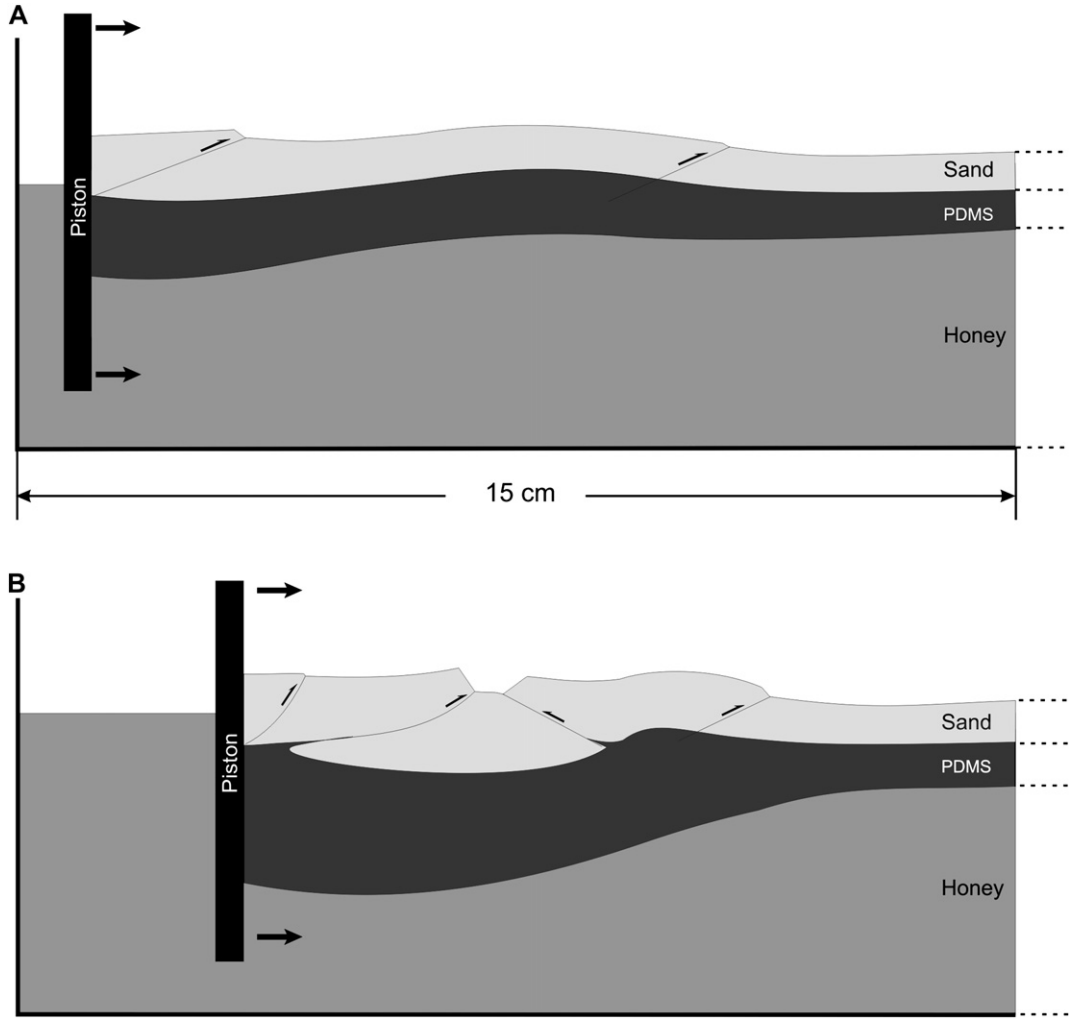

Fig. 5. Schematic cross-sections for fault-first mode as marked in Fig. 3B and D. Sections were reconstructed from observations of upper surface of sand, upper surface of PDMS (after removing sand) and side views through transparent walls and translucent honey. (A) Shortening of model resulted in first development of thrust close to piston, followed by thrust wedge thickening and flexure of sand, and concomitant thickening and bending of underlying PDMS. Thin sheets of PDMS were dragged into hanging walls of thrusts. Isostatic compensation and elastic response resulted in the formation of a fore bulge that developed into a buckle with continued deformation. Later, a new fore thrust formed from the forelimb of the buckle. (B) At a later stage, a back thrust formed from the back limb of the buckle, with formation of pop-ups and contractional basins.

4. Discussion

Results of fold-first model show that the experimental wavelength, which scaled up to nature is around 120 km, falls within the wavelength span 100–300 km observed in the NE Indo-Australian plate and reported by Weissel et al. (1980). Because wavelength was measured in an advanced stage of the experiment for more clear observation of the buckles (higher amplitude), it is likely that earlier experimental wavelength, at lower buckle amplification like in nature, was more within the natural wavelength span. The scaled up wavelength of frontal bulges, ca. 180 km, although resulting from both horizontal shortening and vertical loading, also falls within the wavelength span observed in the Indian Ocean. Both results seem to indicate that the scaling and materials used are appropriate to model shortening of the oceanic lithosphere.

It seems relevant for the present experimental results to discuss the evolution of the Argand number (*Ar*) during the experiments, because it relates the stresses caused by gravity and the stresses caused by shortening. In a model like the one presented here, without erosion and sedimentation, the numerator of the *Ar* ratio (stresses related to gravity) should increase with buckle amplification, because of an increase in the vertical dimension. Therefore, for an invariable denominator, *Ar* should increase and, consequently, should the gravity effects. Presumably, this should favour formation of thrusting from a certain stage, because of the simultaneous effects of gravity and shortening. The balance between the two should control deformation style and progression. When thickening reaches a certain amount, less work is needed to make a thrust from an earlier fold than to continue amplification, or to make a new thrust following an older one, than to continue thrust wedge thickening. Thickening in the model crust is the result of combined thrusting, folding and homogeneous thickening of both sand and PDMS (see Koyi et al., 2003 for a discussion of penetrative strain). However, from the experiments one cannot evaluate

the stresses caused by horizontal shortening at each instant, which does not allow for a complete discussion of the effects of variation of *Ar* during the experiments. This has been done for mathematical analysis of large scale folding by e.g. Schmalholz et al. (2002), who concluded that gravity controls the amplification rate in gravity controlled folding mode; the greater the gravity effect, the lower the amplification rate.

Although intended perturbations were not introduced in the original setup (except at the contact with the piston), the final result regarding fold frequency was always very similar, i.e. a similar number of waves was obtained. This means that, for similar model conditions (mostly similar materials, dimensions and identical strain rate), the final result is reproducible. Interestingly, numerical models obtain a similar result although from an initial setup where perturbations are prescribed. The wavelength selection can therefore be studied in more detail in a numerical model.

When discussing thrust initiation in the present experiments, we have to distinguish between (1) timing of thrust/buckle initiation and (2) location of thrust initiation.

4.1. Timing of thrust/buckle initiation

Why does thrusting sometimes precedes and other times follows buckling? We do not have a complete answer to this question at this stage, but the experiments suggest that it could be related to the initial perturbation in the sand layer at the contact with the piston. Following the idea of Kuenen and de Sitter (1938), a slightly bent layer is less prone to be broken up by shearing planes in the early stages of shortening than a perfectly straight one orthogonal to piston. Therefore, if the layers are flat and horizontal close to the vertical piston, it is easier to generate faults in the early stages. Otherwise it is easier to buckle by amplification of original (though non-intentional) perturbations. Our interpretation follows that of Kuenen and de Sitter (1938) and stems from the experimental set-up. This only depends on how the used materials react to form one or the other first, or even both at the same time. However, the present experimental set up is not appropriate to go into this kind of fine detail. But it is enough to show how thrusts propagate in an isostatically compensated model. At a certain stage, the main thrust is taking up most (if not all) of the applied shortening. Then why does a new thrust form ahead? If the underthrusted material were denser (or became denser), a subduction zone would initiate and there would be no need for development of new thrusts (e.g. Shemenda, 1992). But the underthrusted material has low density, thus upward buoyancy forces arise and play an important role. As movement continues along one thrust, the fault surface and buoyancy forces increase and it gradually begins to lock, despite the weakening effect of PDMS migration up along the fault plane. Thickness of sand almost doubles, the thrust wedge becomes stronger and it starts acting as a natural indenter (see also Marques and Cobbold, 2002, 2006). In terms of Ar, we could say that gravity effects increase to hamper thrusting movement; hence less work is needed to start a new thrust ahead. Then, piston induced displacement propagates beyond the locked thrust and a new cycle begins. Buckling following thrusting can be explained by thrust wedge thickening, which induces downwards flexure of the model lithosphere in the footwall (isostatic compensation) and asymmetric, piston facing upward bulging ahead of the thrust. This bending works as perturbation that facilitates buckle amplification. A distinction is made here between buckling and bulging, because buckling is related to shortening and bulging to load of the thrust slice. In the fault-first type of evolution, bulging seems to precede buckling.

Gerbault et al. (1999) suggested that faults (reverse) can trigger buckling under compression, but previous equivalent experimental work (e.g. Gerbault et al., 1999) shows the opposite. The present experiments show that thrust faults can trigger folding, but the asymmetry and heterogeneity that characterize the experiments (asymmetric buckles and thrusts, and heterogeneous distribution of deformation) is not comparable with the symmetry (conjugate reverse faults) and regularity of spaced faults and buckles with similar wavelength and amplitude observed in the numerical model (e.g. Fig. 2 of Gerbault et al., 1999). The numerical models manage to visualise areas where brittle faulting initiates, in localised or diffuse manner. Diffuse faulting in sand may exist but cannot be detected with the naked eye, and could in part be responsible for homogeneous thickening. In the analogue model, faulting occurrence can only be detected when it is enough localised and developed.

4.2. Location of thrust initiation

In the experiments, thrust initiation took place in buckles' forelimb and back-limb, at a location that is very difficult to pin point because opaque materials were used. While investigating the folding of a cake of plastic clay, Kuenen and de Sitter (1938) observed that faults formed in both limbs of a fold, in particular thrust faults in the forelimb. These thrusts dipped towards the antiformal fold core. However, the authors did not give an exact location for thrust initiation or put forward a mechanical explanation. Cobbold and Davy (1988), Davy and Cobbold (1991), Cobbold et al. (1993), Burg et al. (1994) and Gerbault (2000) suggested that thrust faults initiated at inflection points of forelimbs of buckles, but they also did not pin point the exact location or put forward a mechanical explanation.

The present experiments do not allow locating the initiation point exactly, because sand is not transparent and sidewall views are not that detailed (blurring due to sand friction and silicone drag). But we know from views of the silicone surface, after sand removal, that most thrust faults initiated somewhere around the inflection point of the buckle's forelimb. A mechanical interpretation for initiation and localization of thrusts in the forelimb is illustrated in Fig. 6. Gravitational forces tend to flatten out all layers and make them parallel; the viscous ones more rapidly. Therefore, gravity (vertical component) works against buckling produced by horizontal (tectonic) compression (e.g. Biot, 1961; Ramberg, 1964; Ramberg and Stephansson, 1964). As shown in Fig. 6, gravity tends to flatten the buckled layer because synforms are affected by a buoyant force and antiforms are burdened by excess weight.

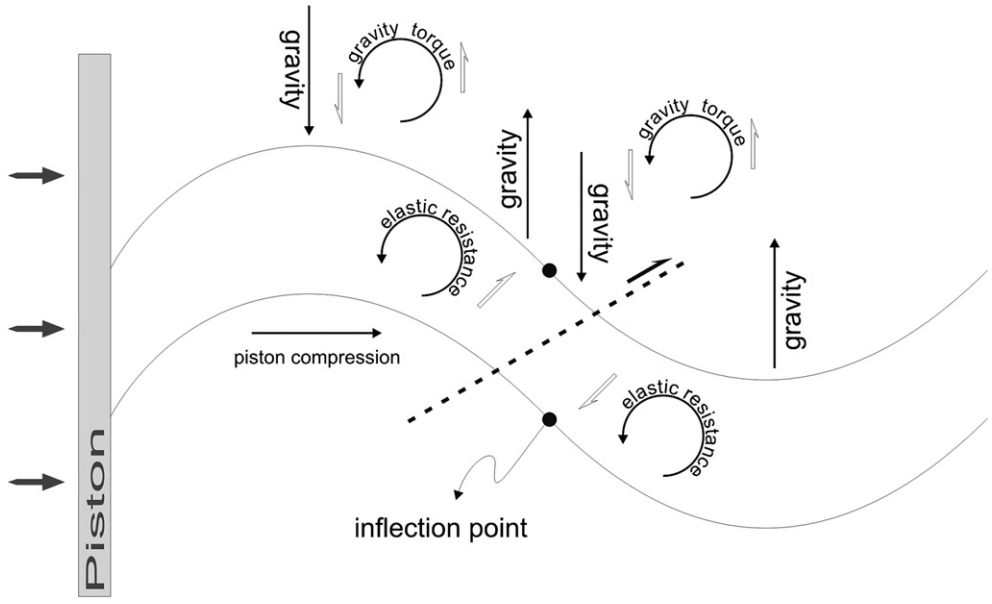

Fig. 6. Schematic representation of forces and torques acting on the model layers. Buckles form and amplify by layer parallel shortening induced by piston displacement (tectonic forces), but gravity and elastic resistance tend to flatten them out. This resistance to amplification and the respective torques make the brittle sand layer to break in the middle of the forelimb if stresses exceed the brittle yield of the sand layer. The horizontal forces also add to thrust movement.

This flattening generates torques in the same limb of both antiform and synform, with identical sign. Therefore, they induce shear. The stored elastic strain also generates torques, with identical sign, in the same limb but to each side of the inflection points. Therefore, they induce shear, which adds to the shear generated by gravity torques. The torques from gravitational and elastic resistance add effects to make the layer flat, and both must be overcome by horizontal compression in order to amplify the buckle. However, if those torques sum up to a significant magnitude, which added to horizontal compression are enough to break the brittle layer, then a thrust fault should form in between the inflection points and dip about 30°, as shown in Fig. 6. Again, it would be relevant to discuss here the evolution and effects of *Ar* for thrust evolution and propagation, because the thrust wedge thickens considerably with shortening. However, information lacks regarding the stresses caused by horizontal shortening and vertical thickening.

Lambeck (1983), using gravity in his mathematical analysis, showed that the inflection point is the locus where the stress differences are at a maximum and can generate a thrust fault.

4.3. Future investigation

For further investigation of this topic, and towards more quantifiable results, we envisage doing experiments in a laboratory with equipment that allow looking inside sand and PDMS (e.g. tomography), and also rigorously measure evolution of topography.

5. Conclusions

The analogue experiments show the following. (1) Thrust initiation may occur in two main modes: fold-first or fault-first. They seem to be the result of presence or absence of significant initial perturbations, respectively. The fault-first mode eventually goes into a fold-first mode due to isostatic compensation in the model and rheological behaviour of the used materials The buckles in the fold-first mode form regularly spaced and simultaneously, in contrast with the buckles in the fault-first mode, which form one at a time from bulges originated in front of new thrusts. (2) In the present models, thrusts usually initiated in the forelimb of buckles as a result of tectonic (horizontal), gravitational (vertical) and elastic forces. (3) Thrust propagation occurred by thrust thickening and downwards flexure due to isostatic compensation, which originated forward formation of bulges and subsequent amplification by buckling. Continued shortening created new thrusting. (4) Bulging ahead of thrusts tended to develop into asymmetric buckles with the shorter limb steeper towards the piston. (5) As a whole, thrust initiation, evolution and propagation seem to depend mostly on how stresses evolve and propagate through the model, and how material strength varies with progressive deformation. The main stresses at play are born at the moving piston (model horizontal tectonic forces), from thickening and isostatic compensation in the model (gravitational forces, e.g. Artyushkov, 1973; Fleitout and Froidevaux, 1983; England and Jackson, 1989; Coblentz et al., 1994; Schmalholz et al., 2002; Marques and Cobbold, 2002, 2006), and from elastic resistance to buckling.

Acknowledgments

This is a contribution to Project TEAMINT (POCTI/CTA/48137/2002) funded by FCT. The experiments were carried out at Géosciences-Rennes, where Jean-Jacques Kermarrec provided technical assistance. This work benefited from discussions with Peter Cobbold. Thorough reviews by Gerbault, Storti, Koyi and Corti helped to considerably improve the quality of this article, and so did the editorial work of J. Hippertt.

References

Artyushkov, E.V., 1973. Stresses in the lithosphere caused by crustal thickness inhomogeneities. Journal of Geophysical Research 78, 7675–7708.

Biot, M.A., 1961. Theory of folding of stratified viscoelastic media and its implications in tectonics and orogenesis. Geological Society of America Bulletin 72, 1595–1620.

Burg, J.-P., Podladchikov, Yu., 1999. Lithospheric scale folding: numerical modelling and application to the Himalayan syntaxes. International Journal of Earth Sciences 88, 190–200.

Burg, J.P., Davy, P., Martinod, J., 1994. Shortening of analogue models of the continental lithosphere: New hypothesis for the formation of the Tibetan plateau. Tectonics 13, 473–483.

Carter, N.L., Tsenn, M.C., 1987. Flow properties of continental lithosphere. Tectonophysics 136, 27–63.

Cloetingh, S., Wortel, R., 1986. Stress in the Indo-Australian plate. Tectonophysics 132, 49–67.

Cloetingh, S., Burov, E., Poliakov, A., 1999. Lithosphere folding: Primary response to compression? (from central Asia to Paris basin). Tectonics 18, 1064–1083.

Cobbold, P.R., Davy, P., Gapais, D., Rossello, E.A., Sadybakasov, E., Thomas, J.C., Tondji Biyo, J.J., de Urreiztieta, M., 1993. Sedimentary basins and crustal thickening. Sedimentary Geology 86, 77–89.

Cobbold, P.R., Davy, P., 1988. Indentation tectonics in nature and experiment. 2. Central Asia. Bulletin of the Geological Institutions of Uppsala. New Series 14, 143–162.

Coblentz, D.D., Richardson, R.M., Sandiford, M., 1994. On the gravitational potential of the Earth's lithosphere. Tectonics 13, 929–945.

Davy, P., Cobbold, P.R., 1988. Indentation tectonics in nature and experiment. 1. Experiments scaled for gravity. Bulletin of the Geological Institutions of Uppsala. New Series 14, 129–141.

Davy, P., Cobbold, P.R., 1991. Experiments on shortening of a 4-layer model of the continental lithosphere. Tectonophysics 188, l–25.

England, P., Jackson, J., 1989. Active deformation of the continents. Annual Review of Earth and Planetary Sciences 17, 197–226.

Fleitout, L., Froidevaux, C., 1983. Tectonic stresses in the lithosphere. Tectonics 2, 315–324.

Gerbault, M., 2000. At what stress level is the central Indian Ocean lithosphere buckling? Earth and Planetary Science Letters 178, 165–181.

Gerbault, M., Burov, E.B., Poliakov, A.N.B., Daignières, M., 1999. Do faults trigger folding in the lithosphere? Geophysical Research Letters 26, 271–274.

Goetze, C., Evans, B., 1979. Stress and temperature in the bending lithosphere as constrained by experimental rock mechanics. Geophysical Journal of the Royal Astronomical Society 59, 463–478.

Hubbert, M.K., 1937. Theory of scale models as applied to the study of geologic structures. Geological Society of America Bulletin 48, 1459–1520.

Hubbert, M.K., 1951. Mechanical basis for certain familiar geologic structures. Geological Society of America Bulletin 62, 355–372.

Kirby, S.H., 1983. Rheology of the lithosphere. Reviews of Geophysics and Space Physics 21, 1458–1487.

Koyi, H.A., Hessami, K., Teixell, A., 2000. Epicenter distribution and magnitude of earthquakes in fold-thrust belts: insights from sandbox models. Geophysical Research Letters 27, 273–276.

Koyi, H.A., Sans, M., Teixell, A., Cotton, J., Zeyen, H., 2003. The significance of penetrative strain in the restoration of shortened layers—Insights from sand models and the Spanish Pyrenees. In: McClay, K.R. (Ed.), Thrust Tectonics and Hydrocarbon Systems. AAPG Memoir 82, pp. 1–16.

Krantz, R.W., 1991. Measurements of friction coefficients and cohesion for faulting and fault reactivation in laboratory models using sand and sand mixtures. Tectonophysics 188, 203–207.

Kuenen, Ph.H., de Sitter, L.U., 1938. Experimental investigation into the mechanism of folding. Leidsche Geol. Med. 10, 217–239.

Kusznir, N.J., Park, R.G., 1982. Intraplate lithosphere strength and heat flow. Nature 299, 540–542.

Lambeck, K., 1983. Structure and evolution of the intracratonic basins of central Australia. Geophysical Journal Royal Astronomical Society 74, 843–886.

Marques, F.O., Cobbold, P.R., 2002. Topography as a major factor in the development of arcuate thrust belts: Insights from sandbox experiments. Tectonophysics 348, 247–268.

Marques, F.O., Cobbold, P.R., 2006. Effects of topography on the curvature of fold-and-thrust belts during shortening of a 2-layer model of continental lithosphere. Tectonophysics 415, 65–80.

Martinod, J., Davy, P., 1994. Periodic Instabilities during compression of the lithosphere: 2. Analogue experiments. Journal of Geophysical Research 99, 12057–12069.

McAdoo, D., Sandwell, D., 1985. Folding of oceanic lithosphere. Journal of Geophysical Research 90, 8563–8569.

Ramberg, H., 1964. Selective buckling of composite layers with contrasted rheological properties, a theory for simultaneous formation of several orders of folds. Tectonophysics 1, 307–341.

Ramberg, H., Stephansson, O., 1964. Compression of floating elastic and viscous plates affected by gravity, a basis for discussing crustal buckling. Tectonophysics 1, 101–120.

Schmalholz, S.M., Podladchikov, Y.Y., Burg, J.-P., 2002. Control of folding by gravity and matrix thickness: Implications for large-scale folding. Journal of Geophysical Research 107, B1, doi:10.1029/2001JB000355.

Shemenda, A.I., 1992. Horizontal lithosphere compression and subduction: Constraints provided by physical modelling. Journal of Geophysical Research 97, 11097–11116.

Sokoutis, D., Burg, J.P., Bonini, M., Corti, G., Cloetingh, S., 2005. Lithospheric-scale structures from the perspective of analogue continental collision. Tectonophysics 406, 1–15.

Stephenson, R.A., Cloetingh, S., 1991. Some examples and mechanical aspects of continental lithospheric folding. Tectonophysics 188, 27–37.

Vening-Meinesz, F.A., 1958. Chapter 10. In: Heiskanen, W.A., Vening-Meinesz, F.A. (Eds.), The Earth and its Gravity Field. McGraw Hill, New York.

Weijermars, R., 1986. Flow behaviour and physical chemistry of bouncing putties and related polymers in view of tectonic laboratory applications. Tectonophysics 124, 325–358.

Weissel, J., Anderson, R.N., Geller, C., 1980. Deformation of the Indo-Australian plate. Nature 287, 284–291.